Final Draft

of the original manuscript

Golub, M.; Lokstein, H.; Soloviov, D.; Kuklin, A.; Wieland, D.; Pieper, J.:

Light-Harvesting Complex II Adopts Different Quaternary Structures in Solution as Observed Using Small-Angle Scattering.

In: The Journal of Physical Chemistry Letters. Vol. 13 (2022) 5, 1258 - 1265.

First published online by ACS: 28.01.2221

https://dx.doi.org/10.1021/acs.jpclett.1c03614

Light-Harvesting Complex II Adopts Different Quaternary Structures in Solution as Observed by Small Angle Scattering

Maksym Golub[a], Heiko Lokstein[b], Dmytro Soloviov[c,d,e], Alexander Kuklin[c,d], D.C. Florian Wieland[f], and Jörg Pieper[a*]

[a] *Institute of Physics, University of Tartu, Wilhelm Ostwald str. 1, 50411 Tartu, Estonia*

[b] *Department of Chemical Physics and Optics, Charles University, Ke Karlovu 3, 121 16 Prague, Czech Republic*

[c] *Joint Institute for Nuclear Research, Dubna, Russia*

[d] *Moscow Institute of Physics and Technology, Dolgoprudny, Russia*

[e] *Institute for Safety Problems of Nuclear Power Plants NAS of Ukraine, Kyiv, Ukraine*

[f] *Helmholtz Zentrum Geesthacht, Institute for Materials Research, Department for Metallic Biomaterials, 21502 Geesthacht*

*Author to whom correspondence should be addressed:

Jörg Pieper
Institute of Physics, University of Tartu, W. Ostwald str. 1, 50411 Tartu, Estonia.

phone.: +(372) 737 4627

fax: +(372) 738 3033

email: pieper@ut.ee

Abstract

The high-resolution crystal structure of the trimeric major light-harvesting complex of photosystem II (LHCII) is often perceived as the basis for understanding its light-harvesting and photoprotective functions. However, the LHCII solution structure as well as its oligomerization or aggregation state may generally differ from the crystal structure and, moreover, also depend on its functional state. In this regard, small angle scattering experiments provide the missing link by offering structural information in aqueous solution at physiological temperatures. Here we use small angle scattering to investigate the solution structures of two different preparations of solubilized LHCII employing the non-ionic detergents n-octyl-β-D-glucoside (OG) and n-dodecyl-β-D-maltoside (β-DM). The data reveal that the LHCII–OG complex is equivalent to the trimeric crystal structure. Remarkably, however, we observe a stable oligomer comprising three LHCII trimers in the case of the LHCII-β-DM preparation implying additional pigment-pigment interactions. The latter complex is assumed to mimic trimer-trimer interactions which play an important role in the context of photoprotective non-photochemical quenching.

Photosynthetic light-harvesting complexes (LHCs) are pigment-protein complexes evolved to collect solar radiation and to transfer resulting excitation energy to the photochemically active reaction centers (for reviews see e.g. [1], [2], [3]). The trimeric light-harvesting complex II (LHCII) is the major antenna complex of green plants and algae. Its structure is well characterized by X-ray crystallography [4, 5] revealing 14 chlorophylls (Chls) and four carotenoids (xanthophylls, oxygen derivatives of carotenes) bound per apo-protein monomer. Center-to-center distances between Chls in the order of only 8-10 Å suggest sizeable excitonic interactions between the pigments to enable efficient excitation energy transfer (EET) [6-9]. In contrast, a previous medium-resolution structure [10] had suggested rather weak excitonic delocalizations in Chl heterodimers [11, 12]. Trimeric LHCII comprises various combinations of the different apo-proteins Lhcb1-3, which are characterized by weakly variant spectroscopic properties [13, 14].

While the crystal structure of LHCII is well known at almost atomic resolution, it is important to keep in mind that spectroscopic studies on light-harvesting functions are usually carried out using samples in solution. It is likely that solubilized membrane proteins may - in general - have different structural features than proteins in crystals. For example, small angle neutron scattering (SANS) indicated slightly larger *ab initio* structures of Photosystems I (PSI) [15] and II (PSII) [16] in solution at physiological temperatures compared with the corresponding X-ray crystal structures. This was explained by increased flexibility of PSI and PSII in solution [15, 16]. In the case of LHCII, molecular dynamics simulations suggest that different structural domains of LHCII including the stromal loop, and, especially, the N-terminus may deviate from the crystal structure [17]. Furthermore, structural differences between solubilized membrane proteins and protein crystal structures were observed using solution nuclear magnetic resonance (NMR) spectroscopy [18, 19]. NMR was also used to determine the solution structures of solubilized LHCII in light harvesting and quenched states [20], in which the quenched state was induced by extracting the detergent form the buffer solution during the sample preparation. A comparison of the two NMR structures revealed altered interactions between certain Chls *a* and neoxanthin as well as Chl-lutein interactions in the

dissipative state. Similar observations were made using non-linear spectroscopic techniques [21]. It also appears that Chls exhibit increased flexibility in unquenched, detergent-solubilized LHCII at physiological temperatures [20]. This is in line with results of quasielastic neutron scattering (QENS) data indicating a drastic increase of protein dynamics towards room temperature due to availability of additional conformational substates [22, 23].

It is also important to note that application of different detergent types to extract and stabilize LHCII from thylakoid membranes leads to different spectroscopic characteristics [24]. For example, protein stability may be affected in the presence of detergent molecules by disrupting protein-protein, pigment-protein and protein-lipid interactions [18, 25-28]. Therefore, the choice of an optimal detergent to solubilize LHCII becomes a critical task to maintain a functionally active, native-like structure for *in vitro* biophysical studies.

In addition to possible deviations between crystal and solution structures, LHCII also displays a remarkable structural flexibility *in vivo* [29], so that - depending on its functional state - oligomerization or aggregation state may play an important role. For example, inevitable fluctuations of light intensity in nature often cause "overload" of the reaction centers' (RCs') capacity leading to potential damage [30]. It was shown that aggregation of LHCII leads to a pronounced decrease in Chl fluorescence yield and lifetime and is thus assumed to mimic the major photoprotective mechanism against excess excitation denoted as non-photochemical quenching (NPQ) [21, 31-41]. The molecular details of NPQ are still subject of an intense scientific debate [29, 42]. There may be different mechanisms including quenching via the first excited singlet state (S_1) of lutein [39, 43] via a Chl–Chl charge transfer state [42, 44] or via other channels [45-47]. In addition, CD spectra of LHCII aggregates and of unstacked thylakoid membranes were found to be very similar, emphasizing the importance of trimer-trimer interactions *in-vivo* [48]. Electron microscopy studies assessed mutual distances between LHCII in membranes [49]. It was suggested that in the NPQ state the average inter-trimer distances can become significantly shorter, implying the establishment of

protein clusters resembling LHCII aggregates *in vitro* [50-52].

Therefore, the question of oligomerization and/or aggregation of LHCII depending on isolation protocol and on detergent type is of great importance. Small angle neutron and X-ray scattering (SANS and SAXS, respectively) have proven to be appropriate experimental techniques to study the latter questions. The use of the small angle scattering techniques provides access to unique structural information on shape, domain organization and aggregation interactions of biomolecules in solution [53-55]. The combination of SAXS and SANS techniques is widely used to study large, flexible and glycosylated proteins, to which high resolution structural techniques, such as crystallography and NMR cannot be easily applied. SANS and SAXS have also been successfully employed in photosynthesis research [56, 57]. For example, neutron studies of plant thylakoid membranes have revealed a size of the grana unit-cell of 157 Å in solution [58, 59], the hydration dependence of PS II membrane spacing [60], the structural arrangement of cyanobacterial thylakoid membranes [61, 62], but also on state transitions in *Chlamydomonas reinhardtii* [56]. SANS is especially powerful to determine solution structures of assemblies of pigment-protein complexes [63]. In addition, SANS was also used to characterize the solution structure of LHCII, [51] PsbO from cyanobacterial PSII [64, 65], the bacterial light-harvesting complex LH2 in solution at physiological temperatures [66] and of trimeric PSI [67, 68].

In this study, we investigate the solution structure of solubilized LHCII using two different preparation protocols employing the non-ionic detergents – n-octyl-β-D-glucoside (OG) and n-dodecyl-β-D-maltoside (β-DM), respectively. Both detergents are widely used to solubilize membrane proteins [65, 69], but may influence the protein stability and affect protein-protein interactions. In addition, following Voigt et al. [21] we address the influence of the detergent concentration on the oligomerization and aggregation state of LHCII.

Solution Structure of the LHCII-OG complex: In a first step, the structure of LHCII in a water-based solution of OG at a detergent concentration of 1.8 % as previously used by Cardoso et al. [65] was investigated by SAXS measurements at the NanoStar instrument at room temperature. Figure 1 shows the scattering intensity of the LHCII-OG sample as a function of scattering vector q. The protein concentration in the sample solution was about 1 mg/ml in order to minimize protein-protein interactions. The SAXS curve of the LHCII-OG sample indicates that the sample is virtually free of aggregation. This is corroborated by the Guinier plot of the measured SAXS curve presented in the inset of Figure 1, which shows the expected linearity for q-values below 0.0015 $Å^{-2}$. The slope of the linear range yields a radius of gyration R_g equal to 31.2 ± 1 Å which is in good agreement with previous results [65]. Furthermore, the SAXS curve of the LHCII-OG sample exhibits a pronounced peak with a maximum at a q-value of about 0.18 $Å^{-1}$(Figure 1). The latter peak corresponds to a small particle with an average radius size of about 25-35 Å. Thus, we assume that this feature of the scattering profile corresponds to free OG micelles. Accordingly, we applied a model to fit the SAXS data of the LHCII-OG complex consisting of two components: i) a cylinder model representing the LHCII – detergent complex (see the red solid line in Figure 1), and ii) a spherical core-shell model accounting for the free OG micelles (see the blue dotted line in Figure 1). Table I provides the fitting parameters of the combined model, which satisfactorily describes the SAXS data including the separate peak at q ~0.18 $Å^{-1}$ (see Figure 1). According to this analysis, LHC II-OG complexes are characterized by a cylinder radius of about 43 Å and by a height of about 50 Å. Especially, the latter value appears to be consistent with the thickness of the thylakoid membrane, into which native LHC II is embedded [4, 5, 56, 59]. The outer radius of the OG micelles is found to be about 28 Å.

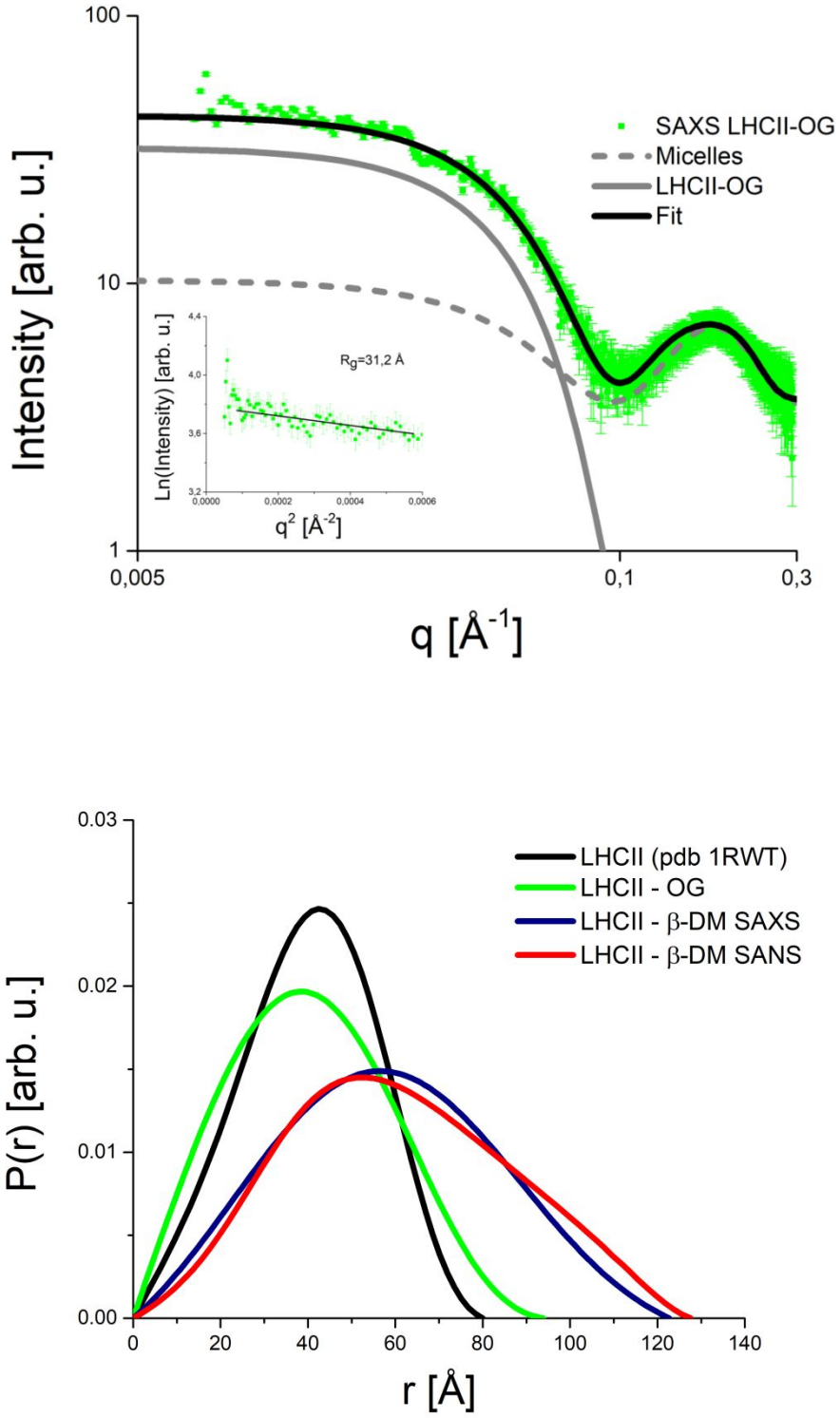

Figure 1, upper panel. SAXS data of LHCII-OG complexes (green dots) in aqueous solution. The grey solid line represents the contribution of the LHCII–OG complex, while the grey dashed line gives the contribution of the free OG micelles. The black line is the overall fitting curves, which is a linear superposition of the two components. The inset shows the Guinier region of the measured SAXS curve with a linear fit according to the eq. (1). The resulting Rg is equal to 31.2 Å. **Lower panel.** Pair-distance distribution functions P(r) obtained from SAXS and SANS experiments in this study. The green curve shows the P(r) functions calculated using Gnom from the LHC II–OG SAXS data; the blue curve represents the P(r) function for the case of the LHCII–β-DM SAXS data and the red line LHCII–β-DM SANS data in 100% D_2O. For comparison, we also present the P(r) function (black line) calculated from the crystal structure of LHCII (1RWT). [4]

Table I. Fitting parameters for SAXS curves of LHCII–OG and LHCII – β-DM using a superposition model.

Cylinder	LHCII–OG SAXS	LHCII–β-DM SAXS	LHCII – β-DM SANS 100% D_2O
Data is shown in	Figure 1	Figure 5B	Figure 5A
Scaling factor A	0.5±0.05	1.1±0.05	0.00135±0.0005
R_{cyl} (Å)	43±5	62±5	62±5
L (Å)	50±8	50±8	50±8
ρ_{cyl} (10^{-6} Å^{-2})	11	11	3
ρ_{solv} (10^{-6} Å^{-2})	9.46	9.46	6.36
Spherical core-shell	OG micelle	β-DM micelle	β-DM micelle
Scaling factor B	83.7±1	103±1	0.00001±0.000005
r_{core} (Å)	13.6±4	13.8±4	13.8±4
r_{sphere} (Å)	28,1±4	30.8±4	30.8±4
ρ_{core} (10^{-6} Å^{-2})	8.75	8.75	-0.1
ρ_{shell} (10^{-6} Å^{-2})	9.66	9.66	1
ρ_{solv} (10^{-6} Å^{-2})	9.46	9.46	6.36
Power law, $C*q^{-p}$	aggregation		
Scaling factor C (10^{-6})	not used	33±1	not used
p	3	3	3
background (arb. u.)	3.60	3	0.0027
Sqrt(X^2/N)	4.8	1.6	8.2

Figure 1 also shows the corresponding pair-distance distribution function P(r) of the LHCII-OG complex (green line) obtained from an IFT analysis of the experimental SAXS curve. It is important to note that the latter analysis was restricted to the q-range smaller than 0,085 Å^{-1}, where the data are dominated by the scattering of the cylinder component while the contribution of the spherical core-shell is small and widely structureless. The P(r) function of the LHCII-OG complex (green line) has an asymmetrical shape with a peak at 38 Å, while D_{max} is about 94 Å. The latter value is larger than the D_{max} of 80 Å expected from the pdb structure of trimeric LHC II [4, 5]. The

larger experimental value of D_{max} is consistent with the presence of an OG detergent belt around the longest dimension of the LHCII structure.

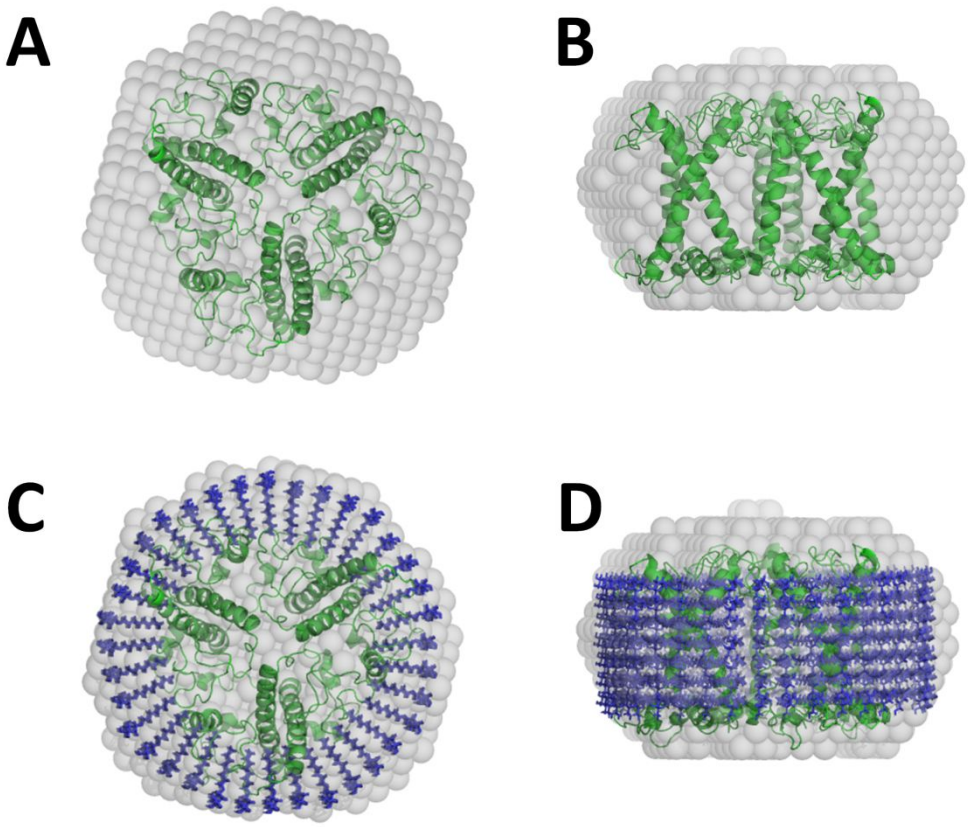

Figure 2: Structure reconstruction of the LHCII–OG complex based on the SAXS data shown in Figure 1. The top (Panels A and C) and lateral (Panels B and D) views are shown with conserved size proportions. The gray spheres correspond to the structure reconstruction of the complex according to the Monte Carlo simulations from the P(r) function using DAMMIF (see Figure 2, green line). The latter structure is superimposed with the LHCII trimer (green) [4]. with an additional detergent belt of OG molecules (blue).

In a next step, we proceed with a structure reconstitution of the LHC II-OG complex using the DAMMIN software routine. Figure 2 shows the top and lateral views of the crystal structure of trimeric LHCII compared with the reconstituted structure (see grey spheres in panels A and B of Figure 2), which corresponds to the experimental P(r) function. A mismatch between the crystal structure of trimeric LHCII and the reconstituted structure is visible in the region of the hydrophobic surfaces of LHCII, which are surrounded by the thylakoid membrane *in vivo*. Thus,

the additional structure can likely be attributed to OG molecules shielding the hydrophobic part of LHCII from the solvent. A single OG molecule has a length of ~15 Å which fits the space suggested by the DAMMIF structure. Panels C and D of Figure 2 show the structure of the LHCII-OG complex assuming a monolayer of OG molecules. We constructed the detergent belt by applying PYMOL[70] and assuming the closest packing of detergent molecules. Based on the above model, it is also possible to estimate the number of OG molecules in the LHCII-OG complex to be about ~250 (7 rows of ~36 OG molecules in a row). Finally, we verified the structure of the LHCII-OG complex as shown in Figure 2 by creating a modified pdb structure including the OG-belt and by using CRYSOL to calculate a theoretical SAXS curve. The latter curve compares well with the experimental SAXS data of Figure 1 (not shown) and thus finally corroborates our model of the whole LHCII-OG complex, which is consistent with the trimeric form of LHCII as in ref.[65].

Solution Structure of the LHCII-β-DM super complex: The solution structure of the LHCII–β-DM complex was investigated using SANS experiments at the YuMo instrument. The concentration of β-DM in the buffer solution was about 0.03%, which is above the critical micelle concentration of ~ 0.01%. However, the concentration of β-DM was significantly lower than the concentration of OG in the SAXS experiment discussed above, where we observed isolated LHCII-trimers. The choice of the initial β-DM concentration was based on previous measurements on isolated LHCII with β-DM using nonlinear polarization spectroscopy [21]. In the latter study, it was inferred indirectly from spectroscopic data that commonly used detergent concentrations (around or slightly above the critical micelle concentration) do not lead to complete trimerization of LHCII and residual aggregation persists up to β-DM concentrations of > 0.06%[21].

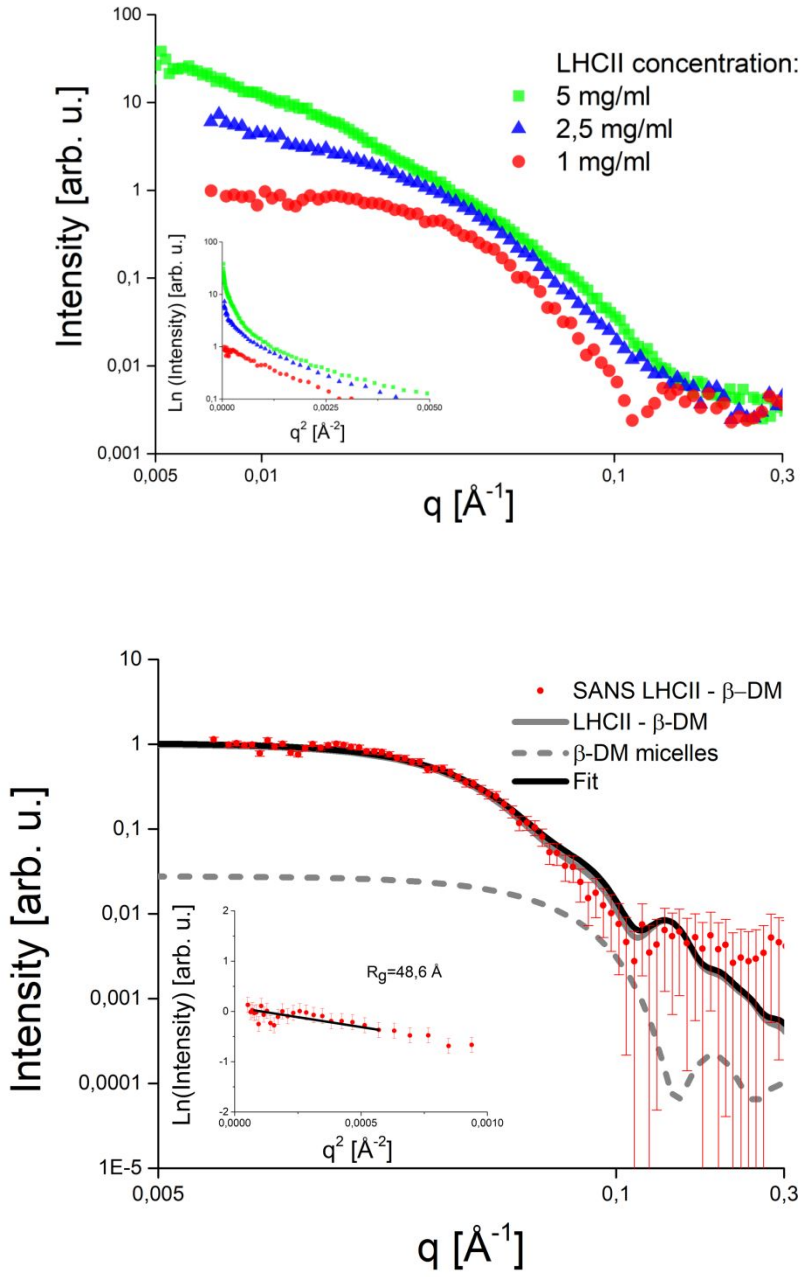

Figure 3, upper panel: SANS data of LHCII-β-DM complexes obtained at different protein concentrations and at a contrast of 100% D_2O. Green dots correspond to the measurement at a protein concentration of 5 mg/ml; blue dots – 2.5 mg/ml and red dots – 1 mg/ml. The inset shows the Guinier plot of the same SANS data. **Lower panel:** SANS data of LHCII (red dots) at the protein concentration of 1 mg/ml in 100% D_2O solution with β-DM (0.03%). The grey solid line represents the contribution of LHCII–β-DM, while the grey dashed line indicates the contribution of β-DM micelles. The black line indicates the final fitting curve, which is linear superposition of the two components. The inset gives the Guinier region of the measured SANS curve with a fit according to the eq. (1). Rg is 48.6 Å.

SANS data directly reveal the oligomerization state of a protein in aqueous solution. Figure 3 shows SANS data of LHC II-β-DM complexes and corresponding Guinier plots for different protein concentrations in 100% D_2O thus representing the entire LHCII–β-DM complex as the SAXS data above. A closer inspection of the SANS data of Figure 3 reveals that the data of the two higher protein concentrations do not tend towards a plateau for decreasing q-values, but rather exhibit a tendency towards an increasing signal with decreasing q. This is a typical signature of protein aggregation. In contrast, a linear behavior in the Guinier region indicating absence of aggregation is present only at the lowest protein concentration of 1 mg/ml (see insert of Figure 3). Remarkably, the experimental Rg of 48.6 Å is pronouncedly higher than the Rg value found for LHCII–OG complexes above (see also Table I).

In order to further investigate the structure of the LHCII–β-DM complexes, we performed a model-depended analysis of the SANS curve at the lowest protein concentration of 1 mg/ml (Figure 3). As above, we applied a model consisting of a cylinder representing the LHCII – detergent complex and of a spherical core-shell accounting for detergent micelles. The fit parameters obtained for the LHCII–β-DM complex are listed in Table I. A comparison with those of the LHCII–OG complex suggests that the cylinder lengths are about 50 Å in all cases and thus again consistent with the transmembrane length of LHC II [4, 5, 56, 59]. However, the cylinder radius of the LHCII–β-DM complex of about 62 Å is significantly larger than in the case of the trimeric LHCII–OG complex. This finding is also supported by the P(r) functions derived from the LHCII–β-DM SANS data (see Figure 1), which are generally shifted towards larger radii compared with the trimeric LHCII–OG complex. The shape of the solution structure of the LHCII–β-DM complex was constructed from the P(r) function shown in Figure 1 using the DAMMIN program. The resulting structure represented by grey spheres in Figure 4 is approximately three times larger than that of the LHCII–OG complexes described above, which indicates the formation of higher order oligomers.

In order to determine the size of the LHCII–β-DM complex, we first assumed an oligomeric structure, in which each LHCII trimer was surrounded by a monolayer β-DM belt as inferred before for the case of PSI trimers by Le et al. [68]. Hence, the interaction between the LHCII–β-DM trimers would be mediated via the β-DM head groups. However, this structure turned out to be too large to fit the measured SANS data (not shown). Instead, a proper fit of the SANS data of the LHCII–β-DM complex required the assumption of an oligomer comprising three LHCII trimers, which is surrounded as a whole by one β-DM belt at the hydrophobic intra-membrane surface of LHCII trimers (see Figure 4). Within the above model, the three interacting LHCII trimers appear to be associated at their hydrophobic regions. In contrast, it was suggested in ref. [4] that the contact between LHCII-digalactosyl diacylglycerol (DGDG) proteoliposomes in the Type III crystal lattice was assumed to be via hydrophilic polar groups of DGDG lipids.

In additional SAXS experiments (see supplementary material), we followed the idea suggested previously to achieve a re-trimerization by increasing the β-DM concentration[21]. However, the super-complex of three LHCII trimers reported above remains stable even at a much higher β-DM concentration of 1.0 % (see Table I and the P(r) function shown in Figure 1).

Turning back to the structural models, Figure 4 shows the structure of the LHCII-β-DM complex, in which β-DM molecules form a monolayer belt that surrounds the hydrophobic part of the three interacting LHCII trimers. A monolayer belt is consistent with our SANS experiments with contrast variation (see supplementary material), but also similar to the β-DM detergent belts of PSI and PSII [16, 69, 71]. This structure of LHCII oligomers with β-DM detergent belt was constructed using PYMOL [70] assuming the closest possible packing of detergent molecules. Based on the latter model, we estimate a number of β-DM molecules in the LHCII–β-DM complex of about 504. Finally, the structure of the LHCII–β-DM complex was verified using CRYSON to calculate the resulting SANS data for the complex with detergent belt. The resulting theoretical curves correspond well to the experimental small angle scattering data (not shown).

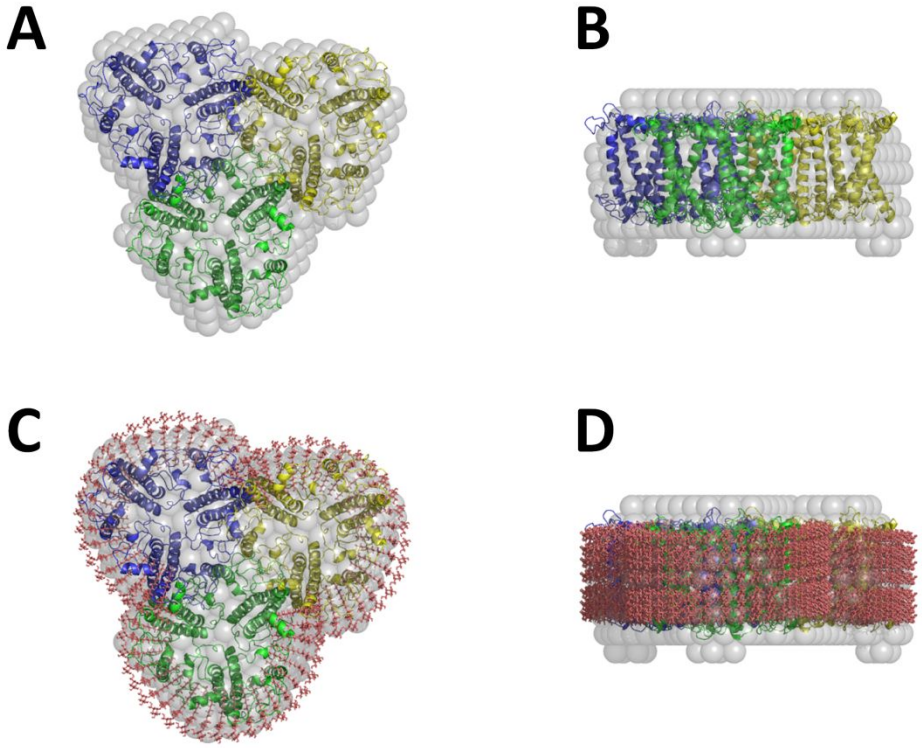

Figure 4: Structure reconstruction of LHCII–β-DM based on SANS and SAXS data. The top (Panels A and C) and lateral (Panels B and D) views are shown next to each other with conserved size proportions. The gray spherical structure is the reconstruction of the complex according to the Monte Carlo simulations from the P(r) function (see Figure 1D, red line). The sphere structure is superimposed with the LHCII oligomer (green, blue and yellow cartoons) with an additional detergent belt of β-DM (red lines).

Implications for functional studies Our combined SANS/SAXS approach directly reveals that LHCII may adopt different quaternary structures in solution depending on preparation method as well as on detergent type and on protein concentration. The LHCII-OG complex is found to be trimeric and similar to the crystal structure, while the LHCII–β-DM complex appears to be an oligomer consisting of three trimers. This shows that the quaternary structure of solubilized LHCII may generally differ from that of its crystal structure giving rise to unexpected inter-trimer pigment-pigment and protein-protein interactions. These results partly corroborate those of Voigt et al. [21], who inferred the presence of higher oligomeric states of LHC II in buffer solution based on the observation of non-linear spectroscopic properties varying with detergent concentration.

Furthermore, our data show that aggregation of the LHCII–β-DM complex can be detected at relatively low protein concentrations. However, a transition from oligomeric structures of the LHCII–β-DM complex to well-separated trimers upon increase of detergent concentration was not reproduced in the present study. Rather, the oligomeric structure of LHCII consisting of three trimers appeared to be quite stable and did not tend to break apart with increasing β-DM concentration. Trimer-trimer interactions of LHCII were also reported based on circular dichroism (CD) data[48] showing that LHCII aggregates isolated according to ref. [72] do not convert to isolated trimers at a β-DM concentration of 0.1%. In contrast, another LHCII–β-DM preparation used for hole burning [73] and neutron scattering experiments [22, 23] was shown to be trimeric by gel filtration chromatography [74]. This indicates that the oligomerization state appears to be determined by preparation method rather than by the detergent used.

Potential implications of trimer-trimer interactions for the spectroscopic properties of LHCII were discussed e.g. by Lambrev et al. [48]. CD data of LHCII aggregates and unstacked thylakoid membranes were found to be very similar, while those of solubilized LHCII differed mainly in the spectral range of carotenoids. The latter study concluded that trimer-trimer interactions might mimic the native organization of LHCII in the thylakoid membrane, where close contacts between LHCII trimers have significant impact on the pigment interactions and may play a role in EET and in the formation of energy-dissipative states [48]. Because solubilized LHCII was shown not to exhibit pigment-pigment interactions stemming from intertrimer interactions, a likely candidate for a pigment affected by the latter intertrimer interactions is neoxanthin, which is largely protruding out of the otherwise rather compact LHCII crystal structure. However, neoxanthin is also in close contact to several Chls including Chl b606 and Chl a604. The latter observation may explain why the CD data of Lambrev et al. [48] do also show smaller differences between solubilized LHCII and aggregates in the Chl spectral range. It is especially interesting, however, that Chl a604 was alternatively proposed to be associated with the lowest energy state of LHCII [9, 73] so that protection against excess excitation energy by NPQ via interaction with neoxanthin at this pigment

site seems to be physiologically important. The LHCII oligomer comprising a trimer of trimers shows that stable complexes mimicking trimer-trimer interactions can be prepared and can be used to study the signatures of corresponding pigment-pigment interactions using spectroscopic techniques.

4. Conclusions

Our combined SANS/SAXS approach provides important insight into structural properties of LHCII in buffer solutions and directly reveals that LHCII may adopt different quaternary structures depending on detergent type and isolation procedure. Especially, we report for the first time that LHCII may form stable nonamers in buffer solution. This suggests that the structure/oligomerization state of LHCII in solution used for spectroscopic studies must not necessarily correspond to that of the high-resolution crystal structures. As a consequence, additional pigment-pigment interactions may arise and open up alternative channels for excitation energy transfer and/or NPQ. It can be anticipated, that the hitherto unknown protein-protein interactions observed here may play a role in the formation of energy-dissipative states of LHCII and constitute a missing link to understand the photoprotective mechanism in LHCII.

Acknowledgements:

Financial support by the Estonian Research Council (Grants PRG 539 and SLOKT 12026 T) is gratefully acknowledged. H.L. gratefully acknowledges financial support by the Charles University Center of Nano- and Bio-Photonics (UNCE/SCI/010) and the Czech Science Foundation, GAČR (grant 20-01159S). We also thank FLNP Dubna for the allocation of beamtime at the YuMO instrument.

References:

1. van Amerongen, H.; Croce, R. In *In Primary Processes of Photosynthesis*, Renger, G., Ed. Cambridge U.K.: 2008.
2. Jankowiak, R.; Reppert, M.; Zazubovich, V.; Pieper, J.; Reinot, T. Site Selective and Single Complex Laser-Based Spectroscopies: A Window on Excited State Electronic Structure, Excitation Energy Transfer, and Electron-Phonon Coupling of Selected Photosynthetic Complexes. *Chem Rev* **2011,** *111*, 4546-4598.
3. Mirkovic, T.; Ostroumov, E. E.; Anna, J. M.; van Grondelle, R.; Govindjee; Scholes, G. D. Light Absorption and Energy Transfer in the Antenna Complexes of Photosynthetic Organisms. *Chem. Rev.* **2017,** *117*, 249-293.
4. Liu, Z.; Yan, H.; Wang, K.; Kuang, T.; Zhang, J.; Gui, L.; An, X.; Chang, W. Crystal Structure of Spinach Major Light-Harvesting Complex at 2.72 a Resolution. *Nature* **2004,** *428*, 287-292.
5. Standfuss, J.; Terwisscha van Scheltinga, A. C.; Lamborghini, M.; Kuhlbrandt, W. Mechanisms of Photoprotection and Nonphotochemical Quenching in Pea Light-Harvesting Complex at 2.5 a Resolution. *EMBO J.* **2005,** *24*, 919-928.
6. Rogl, H.; Schodel, R.; Lokstein, H.; Kuhlbrandt, W.; Schubert, A. Assignment of Spectral Substructures to Pigment-Binding Sites in Higher Plant Light-Harvesting Complex Lhc-Ii. *Biochemistry* **2002,** *41*, 2281-2287.
7. Schubert, A.; Beenken, W. J.; Stiel, H.; Voigt, B.; Leupold, D.; Lokstein, H. Excitonic Coupling of Chlorophylls in the Plant Light-Harvesting Complex Lhc-Ii. *Biophys. J.* **2002,** *82*, 1030-1039.
8. Krikunova, M.; Voigt, B.; Lokstein, H. Direct Evidence for Excitonically Coupled Chlorophylls a and B in Lhc Ii of Higher Plants by Nonlinear Polarization Spectroscopy in the Frequency Domain. *Biochim. Biophys. Acta* **2002,** *1556*, 1-5.
9. Pieper, J.; Irrgang, K. D. Nature of Low-Energy Exciton Levels in Light-Harvesting Complex Ii of Green Plants as Revealed by Satellite Hole Structure. *Photosynth. Res.* **2020,** *146*, 279-285.
10. Kühlbrandt, W.; Wang, D. N.; Fujiyoshi, Y. Atomic Model of Plant Light-Harvesting Complex by Electron Crystallography. *Nature* **1994,** *367*, 614-621.
11. Voigt, J.; Renger, T.; Schödel, R.; Schrötter, T.; Pieper, J.; Redlin, H. Excitonic Effects in the Light-Harvesting Chl a/B-Protein Complex of Higher Plants. *Phys. Status Solidi B* **1996,** *194*, 333-350.
12. Renger, T.; May, V. Simulations of Frequency-Domain Spectra: Structure-Function Relationships in Photosynthetic Pigment-Protein Complexes. *J. Phys. Rev. Lett.* **2000,** *84*, 5228-5231.
13. Standfuss, J.; Kühlbrandt, W. The Three Isoforms of the Light-Harvesting Complex Ii: Spectroscopic Features, Trimer Formation, and Functional Roles. *J Biol Chem* **2004,** *279*, 36884-36891.
14. Irrgang, K. D., Slowik, D., Miao, J., Scharf, K., Wess, M. *Photosynthesis: Fundamental Aspects of Global Perspectives*. Alliance Communications Group: 2005.
15. Midtgaard, S. R.; Darwish, T. A.; Pedersen, M. C.; Huda, P.; Larsen, A. H.; Jensen, G. V.; Kynde, S. A. R.; Skar-Gislinge, N.; Nielsen, A. J. Z.; Olesen, C., et al. Invisible Detergents for Structure Determination of Membrane Proteins by Small-Angle Neutron Scattering. *FEBS J.* **2018,** *285*, 357-371.
16. Golub, M.; Hussein, R.; Ibrahim, M.; Hecht, M.; Wieland, D. C. F.; Martel, A.; Machado, B.; Zouni, A.; Pieper, J. Solution Structure of the Detergent-Photosystem Ii Core Complex Investigated by Small Angle Scattering Techniques. *J. Phys. Chem. B* **2020,** *124*, 8583-8592.
17. Liguori, N.; Periole, X.; Marrink, S. J.; Croce, R. From Light-Harvesting to Photoprotection: Structural Basis of the Dynamic Switch of the Major Antenna Complex of Plants (Lhcii). *Sci. Rep.* **2015,** *5*, 1-10.
18. Danmaliki, G. I.; Hwang, P. M. Solution Nmr Spectroscopy of Membrane Proteins. *Biochim. Biophys. Acta, Biomembr.* **2020,** *1862*, 183356.
19. Gautier, A.; Mott, H. R.; Bostock, M. J.; Kirkpatrick, J. P.; Nietlispach, D. Structure Determination of the Seven-Helix Transmembrane Receptor Sensory Rhodopsin Ii by Solution Nmr Spectroscopy. *Nat. Struct. Mol. Biol.* **2010,** *17*, 768-774.

20. Pandit, A.; Reus, M.; Morosinotto, T.; Bassi, R.; Holzwarth, A. R.; de Groot, H. J. An Nmr Comparison of the Light-Harvesting Complex Ii (Lhcii) in Active and Photoprotective States Reveals Subtle Changes in the Chlorophyll a Ground-State Electronic Structures. *Biochem. Biophys. Acta* **2013,** *1827*, 738-744.
21. Voigt, B.; Krikunova, M.; Lokstein, H. Influence of Detergent Concentration on Aggregation and Spectroscopic Properties of Light-Harvesting Complex Ii. *Photosynth. Res.* **2008,** *95*, 317-325.
22. Vrandecic, K.; Rätsep, M.; Wilk, L.; Rusevich, L.; Golub, M.; Reppert, M.; Irrgang, K.-D.; Kühlbrandt, W.; Pieper, J. Protein Dynamics Tunes Excited State Positions in Light-Harvesting Complex Ii. *J. Phys. Chem. B* **2015,** *119*, 3920-3930.
23. Golub, M.; Rusevich, L.; Irrgang, K. D.; Pieper, J. Rigid Versus Flexible Protein Matrix: Light-Harvesting Complex Ii Exhibits a Temperature-Dependent Phonon Spectral Density. *J. Phys. Chem. B* **2018,** *122*, 7111-7121.
24. Akhtar, P.; Dorogi, M.; Pawlak, K.; Kovacs, L.; Bota, A.; Kiss, T.; Garab, G.; Lambrev, P. H. Pigment Interactions in Light-Harvesting Complex Ii in Different Molecular Environments. *J. Biol. Chem.* **2015,** *290*, 4877-4886.
25. le Maire, M.; Champeil, P.; Möller, J. V. Interaction of Membrane Proteins and Lipids with Solubilizing Detergents. *Biochim. Biophys. Acta* **2000,** *1508*, 86-111.
26. Zhou, Y.; Lau, F. W.; Nauli, S.; Yang, D.; Bowie, J. U. Inactivation Mechanism of the Membrane Protein Diacylglycerol Kinase in Detergent Solution. *Protein Sci.* **2001,** *10*, 378-383.
27. Kurauskas, V.; Hessel, A.; Ma, P.; Lunetti, P.; Weinhaupl, K.; Imbert, L.; Brutscher, B.; King, M. S.; Sounier, R.; Dolce, V., et al. How Detergent Impacts Membrane Proteins: Atomic-Level Views of Mitochondrial Carriers in Dodecylphosphocholine. *J. Phys. Chem. Lett.* **2018,** *9*, 933-938.
28. Chipot, C.; Dehez, F.; Schnell, J. R.; Zitzmann, N.; Pebay-Peyroula, E.; Catoire, L. J.; Miroux, B.; Kunji, E. R. S.; Veglia, G.; Cross, T. A., et al. Perturbations of Native Membrane Protein Structure in Alkyl Phosphocholine Detergents: A Critical Assessment of Nmr and Biophysical Studies. *Chem. Rev.* **2018,** *118*, 3559-3607.
29. Lambrev, P. H.; Akhtar, P. Macroorganisation and Flexibility of Thylakoid Membranes. *Biochem. J.* **2019,** *476*, 2981-3018.
30. Demmig-Adams, B.; Adams, W. W.; Garab, G.; Govindjee Non-Photochemical Quenching and Energy Dissipation in Plants, Algae and Cyanobacteria Preface. *Adv. Photosynth. Resp.* **2014,** *40*, 27-30.
31. Horton, P.; Ruban, A. V.; Rees, D.; Pascal, A. A.; Noctor, G.; Young, A. J. Control of the Light-Harvesting Function of Chloroplast Membranes by Aggregation of the Lhcii Chlorophyll-Protein Complex. *FEBS Lett.* **1991,** *292*, 1-4.
32. Ruban, A. V.; Rees, D.; Noctor, G. D.; Young, A.; Horton, P. Long-Wavelength Chlorophyll Species Are Associated with Amplification of High-Energy-State Excitation Quenching in Higher-Plants. *Biochem. Biophys. Acta* **1991,** *1059*, 355-360.
33. Ruban, A. V.; Horton, P. Mechanism of Delta-Ph-Dependent Dissipation of Absorbed Excitation-Energy by Photosynthetic Membranes .1. Spectroscopic Analysis of Isolated Light-Harvesting Complexes. *Biochem. Biophys. Acta* **1992,** *1102*, 30-38.
34. Ruban, A. V.; Rees, D.; Pascal, A. A.; Horton, P. Mechanism of Delta-Ph-Dependent Dissipation of Absorbed Excitation-Energy by Photosynthetic Membranes .2. The Relationship between Lhcii Aggregation Invitro and Qe in Isolated Thylakoids. *Biochem. Biophys. Acta* **1992,** *1102*, 39-44.
35. Lokstein, H.; Härtel, H.; Hoffmann, P.; Renger, G. Comparison of Chlorophyll Fluorescence Quenching in Leaves of Wild-Type with a Chlorophyll-B-Less Mutant of Barley (Hordeum-Vulgare L). *J. Photochem. Photobiol. B. Biol.* **1993,** *19*, 217-225.
36. Ruban, A. V.; Young, A.; Horton, P. Modulation of Chlorophyll Fluorescence Quenching in Isolated Light-Harvesting Complex of Photosystem-Ii. *Biochim. Biophys. Acta, Bioenerg.* **1994,** *1186*, 123-127.
37. Lokstein, H.; Hartel, H.; Hoffmann, P. Photoprotective Function of Light-Harvesting Complex Ii: A Chlorophyll Fluorescence Study in Leaves of a Wild Type and a Chlorophyll B-Less Mutant of Barley. *Lithuanian J. Physics* **1994,** *34*, 306-312.

38. Ruban, A. V.; Horton, P. The Xanthophyll Cycle Modulates the Kinetics of Nonphotochemical Energy Dissipation in Isolated Light-Harvesting Complexes, Intact Chloroplasts, and Leaves of Spinach. *Plant Physiol.* **1999,** *119*, 531-542.
39. Pascal, A. A.; Liu, Z.; Broess, K.; van Oort, B.; van Amerongen, H.; Wang, C.; Horton, P.; Robert, B.; Chang, W.; Ruban, A. Molecular Basis of Photoprotection and Control of Photosynthetic Light-Harvesting. *Nature* **2005,** *436*, 134-137.
40. Gruszecki, W. I.; Grudzinski, W.; Gospodarek, M.; Patyra, M.; Maksymiec, W. Xanthophyll-Induced Aggregation of Lhcii as a Switch between Light-Harvesting and Energy Dissipation Systems. *Biochim. Biophys. Acta* **2006,** *1757*, 1504-1511.
41. Ruban, A. V. Light Harvesting Control in Plants. *FEBS Lett.* **2018,** *592*, 3030-3039.
42. Ruban, A. V.; Johnson, M. P.; Duffy, C. D. The Photoprotective Molecular Switch in the Photosystem Ii Antenna. *Biochim. Biophys. Acta* **2012,** *1817*, 167-181.
43. Ruban, A. V.; Berera, R.; Ilioaia, C.; van Stokkum, I. H.; Kennis, J. T.; Pascal, A. A.; van Amerongen, H.; Robert, B.; Horton, P.; van Grondelle, R. Identification of a Mechanism of Photoprotective Energy Dissipation in Higher Plants. *Nature* **2007,** *450*, 575-578.
44. Ostroumov, E. E.; Gotze, J. P.; Reus, M.; Lambrev, P. H.; Holzwarth, A. R. Characterization of Fluorescent Chlorophyll Charge-Transfer States as Intermediates in the Excited State Quenching of Light-Harvesting Complex Ii. *Photosynth. Res.* **2020,** *144*, 171-193.
45. Holt, N. E.; Zigmantas, D.; Valkunas, L.; Li, X. P.; Niyogi, K. K.; Fleming, G. R. Carotenoid Cation Formation and the Regulation of Photosynthetic Light Harvesting. *Science* **2005,** *307*, 433-436.
46. Bode, S.; Quentmeier, C. C.; Liao, P. N.; Hafi, N.; Barros, T.; Wilk, L.; Bittner, F.; Walla, P. J. On the Regulation of Photosynthesis by Excitonic Interactions between Carotenoids and Chlorophylls. *Proc. Natl. Acad. Sci. U. S. A.* **2009,** *106*, 12311-12316.
47. Naqvi, K. R.; Javorfi, T.; Melo, T. B.; Garab, G. More on the Catalysis of Internal Conversion in Chlorophyll a by an Adjacent Carotenoid in Light-Harvesting Complex (Ch1a/B Lhcii) of Higher Plants: Time-Resolved Triplet-Minus-Singlet Spectra of Detergent-Perturbed Complexes. *Spectrochim. Acta, Part A* **1999,** *55*, 193-204.
48. Lambrev, P. H.; Varkonyi, Z.; Krumova, S.; Kovacs, L.; Miloslavina, Y.; Holzwarth, A. R.; Garab, G. Importance of Trimer-Trimer Interactions for the Native State of the Plant Light-Harvesting Complex Ii. *Biochim. Biophys. Acta* **2007,** *1767*, 847-853.
49. Ruban, A. V.; Johnson, M. P. Visualizing the Dynamic Structure of the Plant Photosynthetic Membrane. *Nat. Plants* **2015,** *1*, 15161.
50. Johnson, M. P.; Goral, T. K.; Duffy, C. D.; Brain, A. P.; Mullineaux, C. W.; Ruban, A. V. Photoprotective Energy Dissipation Involves the Reorganization of Photosystem Ii Light-Harvesting Complexes in the Grana Membranes of Spinach Chloroplasts. *Plant Cell* **2011,** *23*, 1468-1479.
51. Goral, T. K.; Johnson, M. P.; Duffy, C. D.; Brain, A. P.; Ruban, A. V.; Mullineaux, C. W. Light-Harvesting Antenna Composition Controls the Macrostructure and Dynamics of Thylakoid Membranes in Arabidopsis. *Plant J.* **2012,** *69*, 289-301.
52. Ware, M. A.; Giovagnetti, V.; Belgio, E.; Ruban, A. V. Psbs Protein Modulates Non-Photochemical Chlorophyll Fluorescence Quenching in Membranes Depleted of Photosystems. *J. Photochem. Photobiol. B* **2015,** *152*, 301-307.
53. Jacques, D. A.; Trewhella, J. Small-Angle Scattering for Structural Biology--Expanding the Frontier While Avoiding the Pitfalls. *Protein Sci.* **2010,** *19*, 642-657.
54. Kikhney, A. G.; Svergun, D. I. A Practical Guide to Small Angle X-Ray Scattering (Saxs) of Flexible and Intrinsically Disordered Proteins. *FEBS Lett.* **2015,** *589*, 2570-2577.
55. Franke, D.; Petoukhov, M. V.; Konarev, P. V.; Panjkovich, A.; Tuukkanen, A.; Mertens, H. D. T.; Kikhney, A. G.; Hajizadeh, N. R.; Franklin, J. M.; Jeffries, C. M., et al. Atsas 2.8: A Comprehensive Data Analysis Suite for Small-Angle Scattering from Macromolecular Solutions. *J. Appl. Crystallogr.* **2017,** *50*, 1212-1225.
56. Nagy, G.; Garab, G.; Pieper, J., Neutron Scattering in Photosynthesis Research. In *Contemporary Problems of Photosynthesis* Allakhverdiev, S.; Rubin, A. B.; Shuvalov, V. A., Eds. Institute of Computer Science: Izhevsk, 2014; Vol. 1, pp 69-121.

57. Tiede, D. M.; Thiyagarjan, P., Characterization of Photosynthetic Supramolecular Assemblies Using Small Angle Neutron Scattering. In *Biophysical Techniques in Photosynthesis*, Amesz, J.; Hoff, A. J., Eds. Springer: Netherlands, 1996; Vol. 3, pp 375-390.
58. Kirkensgaard, J. J. K.; Holm, J. K.; Larsen, J. K.; Posselt, D. Simulation of Small-Angle X-Ray Scattering from Thylakoid Membranes. *J. Appl. Crystallogr.* **2009,** *42*, 649-659.
59. Nagy, G.; Posselt, D.; Kovacs, L.; Holm, J. K.; Szabo, M.; Ughy, B.; Rosta, L.; Peters, J.; Timmins, P.; Garab, G. Reversible Membrane Reorganizations During Photosynthesis in Vivo: Revealed by Small-Angle Neutron Scattering. *Biochem. J.* **2011,** *436*, 225-230.
60. Pieper, J.; Rusevich, L.; Hauss, T.; Renger, G. Lamellar Spacing of Photosystem Ii Membrane Fragments Upon Dehydration Studied by Neutron Membrane Diffraction. *Optofluid.* **2015,** *2*, 36-40.
61. Liberton, M.; Page, L. E.; O'Dell, W. B.; O'Neill, H.; Mamontov, E.; Urban, V. S.; Pakrasi, H. B. Organization and Flexibility of Cyanobacterial Thylakoid Membranes Examined by Neutron Scattering. *J. Biol. Chem.* **2013,** *288*, 3632-3640.
62. Li, Y.; Lin, Y.; Garvey, C. J.; Birch, D.; Corkery, R. W.; Loughlin, P. C.; Scheer, H.; Willows, R. D.; Chen, M. Characterization of Red-Shifted Phycobilisomes Isolated from the Chlorophyll F-Containing Cyanobacterium Halomicronema Hongdechloris. *Biochim. Biophys. Acta* **2016,** *1857*, 107-114.
63. Tiede, D. M.; Littrell, K.; Marone, P. A.; Zhang, R.; Thiyagarjan, P. Solution Structure of a Biological Bimolecular Electron Transfer Complex: Characterization of the Photosynthetic Reaction Center-Cytochrome C2 Protein Complex by Small Angle Neutron Scattering. *J. Appl. Crystallogr.* **2000,** *33*, 560-564.
64. Slowik, D.; Rossmann, M.; Konarev, P. V.; Irrgang, K. D.; Saenger, W. Structural Investigation of Psbo from Plant and Cyanobacterial Photosystem Ii. *J. Mol. Biol.* **2011,** *407*, 125-137.
65. Cardoso, M. B.; Smolensky, D.; Heller, W. T.; O'Neill, H. Insight into the Structure of Light-Harvesting Complex Ii and Its Stabilization in Detergent Solution. *J. Phys. Chem. B* **2009,** *113*, 16377-16383.
66. Tang, K. H.; Blankenship, R. E. Neutron and Light Scattering Studies of Light-Harvesting Photosynthetic Antenna Complexes. *Photosynth. Res.* **2012,** *111*, 205-217.
67. O'Neill, H.; Heller, W. T.; Helton, K. E.; Urban, V. S.; Greenbaum, E. Small-Angle X-Ray Scattering Study of Photosystem I-Detergent Complexes: Implications for Membrane Protein Crystallization. *J. Phys. Chem. B* **2007,** *111*, 4211-4219.
68. Le, R. K.; Harris, B. J.; Iwuchukwu, I. J.; Bruce, B. D.; Cheng, X.; Qian, S.; Heller, W. T.; O'Neill, H.; Frymier, P. D. Analysis of the Solution Structure of Thermosynechococcus Elongatus Photosystem I in N-Dodecyl-Beta-D-Maltoside Using Small-Angle Neutron Scattering and Molecular Dynamics Simulation. *Arch. Biochem. Biophys.* **2014,** *550-551*, 50-57.
69. Golub, M.; Hejazi, M.; Kolsch, A.; Lokstein, H.; Wieland, D. C. F.; Zouni, A.; Pieper, J. Solution Structure of Monomeric and Trimeric Photosystem I of Thermosynechococcus Elongatus Investigated by Small-Angle X-Ray Scattering. *Photosynth. Res.* **2017,** *133*, 163-173.
70. DeLano, W. L. *Pymol Molecular Graphics System* 0.99; California U.S.A., 2006.
71. Golub, M.; Kölsch, A.; Feoktystov, A.; Zouni, A.; Pieper, J. Insights into Solution Structures of Photosynthetic Protein Complexes from Small-Angle Scattering Methods. *Crystals* **2021,** *11*, 1-16.
72. Krupa, Z.; Huner, N. P.; Williams, J. P.; Maissan, E.; James, D. R. Development at Cold-Hardening Temperatures : The Structure and Composition of Purified Rye Light Harvesting Complex Ii. *Plant Physiol.* **1987,** *84*, 19-24.
73. Pieper, J.; Rätsep, M.; Irrgang, K. D.; Freiberg, A. Chromophore-Chromophore and Chromophore-Protein Interactions in Monomeric Light-Harvesting Complex Ii of Green Plants Studied by Spectral Hole Burning and Fluorescence Line Narrowing. *J. Phys. Chem. B* **2009,** *113*, 10870-10880.
74. Pieper, J.; Irrgang, K. D.; Renger, G.; Lechner, R. E. Density of Vibrational States of the Light-Harvesting Complex Ii of Green Plants Studied by Inelastic Neutron Scattering. *J. Phys. Chem. B* **2004,** *108*, 10556-10565.

TOC graphics: